astro-ph/0008107
August 2000

Planck-scale deformation of Lorentz symmetry as a solution to the UHECR and the TeV-γ paradoxes

Giovanni AMELINO-CAMELIA[a] and **Tsvi PIRAN**[b]

[a] *Dipart. Fisica, Univ. Roma "La Sapienza", P.le Moro 2, 00185 Roma, Italy*
[b] *Racah Institute of Physics, Hebrew University, Jerusalem 91904, Israel*

ABSTRACT

One of the most puzzling current experimental physics paradoxes is the arrival on Earth of Ultra High Energy Cosmic Rays (UHECRs) with energies above the GZK threshold (5×10^{19}eV). Photopion production by CMBR photons should reduce the energy of these protons below this level. The recent observation of 20TeV photons from Mk 501 (a BL Lac object at a distance of 150Mpc) is another somewhat similar paradox. These high energy photons should have disappeared due to pair production with IR background photons. A common feature of these two paradoxes is that they can both be seen as "threshold anomalies": energies corresponding to an expected threshold (pion production or pair creation) are reached but the threshold is not observed. Several (relatively speculative) models have been proposed for the UHECR paradox. No solution has yet been proposed for the TeV-γ paradox. Remarkably, the single drastic assumption of a violation of ordinary Lorentz invariance would resolve both paradoxes. We present here a formalism for the systematic description of the type of Lorentz-invariance deformation (LID) that could be induced by non-trivial short-distance structure of space-time, and we show that this formalism is well suited for comparison of experimental data with LID predictions. We use the UHECR and TeV-γ data, as well as upper bounds on time-of-flight differences between photons of different energies, to constrain the parameter space of the LID. A model with only two free parameters, an energy scale and a dimensionless parameter characterizing the functional dependence on the energy scale, is shown to be sufficient to solve both the UHECR and the TeV-γ threshold anomalies while satisfying the time-of-flight bounds. The allowed region of the two-parameter space is relatively small, but, remarkably, it fits perfectly the expectations of the quantum-gravity-motivated space-time models known to support such deformations of Lorentz invariance: an integer value of the dimensionless parameter and a characteristic energy scale constrained to a narrow interval in the neighborhood of the Planck scale.

1 Introduction

Significant evidence has accumulated in recent years suggesting that in two different regimes, Ultra High Energy Cosmic Rays (UHECRs) and multi-TeV photons, the universe is more transparent than what it was expected to be. UHECRs interact with the Cosmic Microwave Background Radiation (CMBR) and produce pions. TeV photons interact with the Infra Red (IR) photons and produce electron-positron pairs. These interactions should make observations of UHECRs with $E > 5{\times}10^{19}$eV (the GZK limit) [1] or of gamma-rays with $E > 20$TeV from distant sources unlikely [2, 3, 4]. Still UHECRs above the GZK limit and 20TeV photons from Mk 501 are observed.

Numerous solutions have been proposed for the UHECR paradox (see [5] for a recent review). Most of these solutions require new Physics. There are practically no proposals concerning the TeV-γ paradox (see however, [6]). It is striking that there are some common features in these otherwise apparently unrelated paradoxes. In both cases low energy photons interact with high energy particles. The reactions should take place because when Lorentz transformed to the CM frame the low energy photon have sufficient energy to overcome an intrinsic threshold. In both cases the CM energies are rather modest ($\sim$ 100 MeV for UHECRs and $\sim$ 1 MeV for the TeV photons) and the physical processes involved are extremely well understood and measured in the laboratory. In both cases we observe particles above a seemingly robust threshold and the observations can be considered as a "threshold anomaly". It is remarkable that in spite of these similarities at present there is only one mechanism that could resolve both paradoxes: a mechanism based on the single, however drastic, assumption of a violation of ordinary Lorentz invariance.

The possibility that the cosmic-ray threshold anomaly could be a signal of violation of ordinary Lorentz invariance had already been emphasized in Refs. [7, 8, 9, 10, 11]. In this work we combine these earlier points with the very recent suggestion [12, 13, 14] that Lorentz-invariance violation could be the origin of the TeV-γ threshold anomaly. We analyze a general phenomenological framework for the description of the type of Lorentz-invariance deformation (LID) that could be induced by non-trivial short-distance structure of space-time, and we ask whether there are choices of LID parameters that would simultaneously solve the two threshold anomalies while satisfying the constraints imposed by the fact that the results of experimental searches [15, 16] of energy-dependent relative delays between the times of arrival of simultaneously emitted photons are still consistent with ordinary Lorentz invariance. We obtain, under these assumptions, strict limits on the possible parameter space of LID. The fact that one is at all able to give a quantitative description of both threshold anomalies with a simple two-parameter LID model provides encouragement for the interpretation of the data as a sign of LID; moreover, it is quite remarkable that the values expected from quantum-gravity considerations (most notably the energy scale characterizing the deformation being given by the Planck scale) are in agreement with the strict limits we derive.

We review in Sections 2 and 3 the observational background and the theoretical problems related to the observations of UHECRs (Section 2) and TeV photons (Section 3). In Section 4 we describe a special (two parameter) model for LID and we obtain limits on these two parameters. In Section 5 we describe a more general five-parameter LID formalism and again we constrain the parameter space with the available data. In Section 6 we compare our formalism with the Coleman and Glashow [8] formalism for Planck-scale-independent Lorentz invariance violations. We summarize our results in section 7. Appendix A is devoted to the κ-Minkowski space-time, which is an example of quantum-gravity motivated space-time that allows a simple illustration of some of the structures here considered.

2 UHECRs and the GZK paradox

The high energy cosmic rays (CR) spectrum depicts a clear break at $\sim 5{\times}10^{18}$eV. This break is accompanied by a transition in the CR composition from nuclei to protons. Above this

break the spectrum behaves (with a decreasing statistical certainty due to the small number of events) as a single power law $N(E) \sim E^{-2.7}$ all the way up to 3.2×10^{20}eV [17], the highest energy CR observed so far.

A sufficiently energetic CMBR photon, at the tail of the black body thermal distribution, is seen in the rest frame of an Ultra High Energy (UHE) proton with $E > 5\times10^{19}$eV as a > 140MeV photon, above the threshold for pion production. UHE protons should loose energy due to photopion production and should slow down until their energy is below the GZK energy[1]. The process stops when CMBR photons energetic enough to produce pions are not sufficiently abundant [1]. The proton's mean free path in the CMBR decreases exponentially with energy (down to a few Mpc) above the GZK limit ($\sim 5\times10^{19}$eV). Yet more than 15 CRs have been observed with nominal energies at or above $10^{20}\pm30\%$ eV[18, 19].

There are no astrophysical sources capable of accelerating particles to such energies within a few tens of Mpc from us (at least not in the direction of the observed UHECRs). Furthermore if the CRs are produced homogeneously in space and time, we would expect a break in the CR spectrum around the GZK threshold: below the threshold we would observe CRs from the whole universe; above the threshold we would observe CRs only from the nearest few Mpc. The corresponding jump by a factor of $\sim 30 - 100$ in the extrapolated number counts above and below the threshold, is not seen.

Numerous solutions have been proposed to resolve the GZK paradox (see [5] for a recent review). These solutions include, among others, new physics solutions like the decay of topological defects, weakly interacting messengers like S_0 or neutrinos with anomalous cross sections at high energies (the 'Z-burst" model). Conventional astrophysics solutions like acceleration of UHECRs by GRBs or local AGNs require the ad hoc assumption that Earth is located in a not generic place in space-time (we should be nearer than average to a typical source by a factor of 5) as well as very strong intergalactic magnetic fields [20]. Another conventional solution, the acceleration of Fe nuclei by magnetars in the galactic halo, requires a new, otherwise unobserved, population of galactic halo objects. Clearly there is no simple conservative solution to this puzzle.

From the point of view of our LID phenomenology it is important to notice that for a solution of the GZK paradox it would be necessary (and sufficient) for LID to push the threshold energy upwards by a factor of six. In fact, the mean free path of a 5×10^{19}eV proton is almost a Gpc, while the highest observed UHECR energy is 3.2×10^{20}eV.

3 TeV photons from Mk 501 and Mk 421

HEGRA has detected high-energy photons with a spectrum ranging up to 24 TeV [21] from Markarian 501 (Mk 501), a BL Lac object at a redshift of 0.034 (~ 157 Mpc). This observation indicates a second paradox of a similar nature. A high energy photon propagating in the intergalactic space can interact with an IR background photon and produce an electron-positron pair if the CM energy is above $2m_ec^2$. The maximal wavelength of an IR photon that could create a pair with a 10 TeV photon is $40\mu m$. As the cross section for pair creation peaks at a center of mass energy of about $3m_ec^2$, 10 TeV photons are most sensitive to 30μM IR photon and the mean free path of these photons depends on the spectrum of the IR photons at the $\sim 15 - 40\mu$M range. These wavelengths scale like $10\text{TeV}/E$ for different energies.

[1]The exact composition of UHECRs is unknown and it is possible that UHECRs are heavy nuclei rather than protons. In this case such nuclei would undergo photodisintegration when interacting with CMBR photons. The threshold energy for a photodisintegration of a nuclei is several MeV. It just happens to be true, purely as a result of a numerical coincidence, that the threshold is reached when the energy of a typical nuclei, say Fe, is $\sim 5\times10^{19}$eV. Thus the GZK paradox is insensitive to the question of what is the exact composition of UHECRs.

There have been several attempts to model the IR background resulting from different cosmological evolutionary models [22, 23, 24, 25]. Recently, new data from DIRBE at $2.2\mu M$ [26], at 60 and 100 μM [27] and at 140 and 240 μM [28], and from ISOCOM at 15μM [29] suggest that the IR background is even higher. According to these data the flux of IR photons is $\sim 2.5\times10^{-5}$erg cm^{-2}sec^{-1}sr^{-1} around 60-120 μM and falls off by an order of magnitude towards 15 μM. This decrease is important as it would lead to a much shorter mean free path for 20TeV photons as compared to the mean free path of 10TeV photons.

It was originally suggested that the expected break, corresponding to hard-photon disappearance in the IR background, in the GeV-to-TeV spectrum of AGNs could be used to determine the IR background spectrum. This would have been based on searches of a distance-dependent break in the spectrum of various AGNs. However, no apparent break is seen in the spectrum of MK 501 at $\sim$ 20TeV range, where the optical depth seems to exceed unity. Using current IR background estimates Coppi and Aharonian [30] find an optical depth of 5 for 20TeV photons from MK 501 (see also [14]). This optical depth increases rapidly with energy. Thus, photons at these energies are exponentially suppressed, unless they somehow evade the pair-production process.

Unlike the GZK paradox only a few solutions have been proposed for the TeV-γ paradox. First, it is possible that there is an upturn in the intrinsic spectrum emitted by Mk 501. Such an upturn would compensate for the exponential suppression at this region. Clearly this is an extremely fine-tuned solution as the expected energy of this upturn should somehow be tuned to the energy at which the optical depth from MK 501 to Earth is unity. This energy scale is distance dependent and it puts us in a very special position relative to the source. It is of course possible that the IR intensity has been overestimated. A shift in the energy estimate of HEGRA would also explain the paradox. Finally Harwit, Protheroe and Biermann [6] suggest that multiple TeV photons may be emitted coherently by Mk 501 and if they arrive at Earth very close in time and space they may be confused with a single photon event with higher energy.

With current data, $\sim$ 10TeV photons from Mk 501 could reach Earth, while $\sim$ 20TeV photons are exponentially suppressed. This happens mainly because of the rapid fall off of the IR spectrum below 60μm. We conclude that a LID upwards shift of the threshold energy by a factor of two would resolve this paradox.

Having discussed the relevance of Mk 501 for the emergence of the TeV-γ threshold anomaly we turn now to TeV photons from Mk 421 (another BL Lac object at a redshift of 0.031, corresponding to $\sim$ 143Mpc). It is not clear if the spectrum of this source extends high enough to pose a paradox comparable to the one indicated by Mk 501. However, we note here the simultaneous (within the experimental sensitivity) arrival of 1TeV photons and 2TeV from this source. This was used to limit the time-of-flight differences between photons of different energies to less than 200 seconds. This in turn allowed to establish, through an analysis of the type proposed in Ref. [31], an upper limit on Planck-scale-induced LID [16] which will be a key element of our analysis. We call these constraints in the following time-of-flight constraints.

4 Lorentz-invariance-violating dispersion relation

We start by considering first, a class of dispersion relations (following [32, 33, 31] for $\alpha = 1$, and [34, 35] for a general α) which in the high-energy regime takes the form:

$$E^2 - \vec{p}^2 - m^2 \simeq \eta E^2 \left(\frac{E}{E_p}\right)^\alpha \simeq \eta \vec{p}^2 \left(\frac{E}{E_p}\right)^\alpha \ . \qquad (1)$$

m, E and $\vec{p}$ denote the mass, the energy and the (3-component) momentum of the particle, E_p is the Planck energy scale ($E_p \sim 10^{22}$MeV), while α and η are free parameters characterizing the deviation from ordinary Lorentz invariance (in particular, α specifies how strongly

the magnitude of the deformation is suppressed by E_p). Clearly, in (1) the "speed-of-light constant" c has been set to one. (Note however that in this framework c is to be understood as the speed of low-energy massless particles [31].) Also notice that in (1) we wrote the deformation term in two ways, as a $E^2(E/E_p)^\alpha$ correction and as a $p^2(E/E_p)^\alpha$ correction, which are equivalent within our present analysis based exclusively on high-energy data, for which $E \sim p$, but would be different when studied with respect to low-energy data. (Of course, a given short-distance picture of space-time will have only one dispersion relation; for example, in "κ-Minkowski space-time", the space-time which we describe in Appendix A in order to illustrate in an explicit framework some of the structures relevant for our analysis, one encounters a deformation of type $p^2(E/E_p)^\alpha$.)

In previous works [31-35,9] a slightly different notation had been used to describe this same class of deformations, which in particular replaced our η by two quantities: the scale $E_{QG} \equiv |\eta|^{-1/\alpha} E_p$ and a sign variable $\xi_\pm \equiv \eta/|\eta|$. The α,η notation turns out to be more suitable for the description of the technical aspects of the analysis discussed here, but it is useful to keep in mind that the scale of Lorentz-deformation is obtained as $|\eta|^{-1/\alpha} E_p$.

As hinted by the presence of the Planck scale, our interest in deformed dispersion relations of type (1) originates from the fact that such deformations have independently emerged in theory work on quantum properties of space-time. We postpone the discussion of this motivation to the next Section, where we also clarify which types of generalizations of (1) could also be motivated by Planck-scale physics.

While our analysis is motivated by the role that the deformed dispersion relation (1) might have in quantum gravity, one could of course consider (1) quite independently of quantum gravity[2]. The quantum-gravity intuition would then be seen as a way to develop a theoretical prejudice for plausible values of α and η. In particular, corrections going like $(E/E_p)^\alpha$ typically emerge in quantum gravity as leading-order pieces of some more complicated analytic structures [31, 33, 38, 39]. This provides, of course, a special motivation for the study of the cases $\alpha = 1$ and $\alpha = 2$. [$f(E/E_p) \simeq 1 + a_1 (E/E_p)^{n_1} + ...$] Moreover, the fact that in quantum gravity the scale E_{QG} is expected to be somewhere between the GUT scale and the Planck scale corresponds to the expectation that η should not be far from the range $1 \leq \eta \leq 10^{3\alpha}$.

4.1 Deformed thresholds from deformed dispersion relations

We intend to discuss the implications of Eq. (1) for the evaluation of threshold momenta. Before doing that let us briefly summarize the derivation of the equation describing the threshold in the ordinary Lorentz-invariant case. Relevant for our phenomenological considerations is the process in which the head-on collision between a soft photon of energy ϵ and momentum q and a high-energy particle of energy E_1 and momentum $\vec{p}_1$ leads to the production of two particles with energies E_2,E_3 and momenta $\vec{p}_2$,$\vec{p}_3$. At threshold (no energy available for transverse momenta), energy conservation and momentum conservation imply

$$E_1 + \epsilon = E_2 + E_3 \ , \tag{2}$$

$$p_1 - q = p_2 + p_3 \ ; \tag{3}$$

moreover, using the ordinary Lorentz-invariant relation between energy and momentum, one also has the relations

$$q = \epsilon \ , \quad E_i = \sqrt{p_i^2 + m_i^2} \simeq p_i + \frac{m_i^2}{2p_i} \ , \tag{4}$$

[2]Having mentioned that of course the deformation (1) could be considered independently of its quantum-gravity motivation, let us also mention in passing that even outside the quantum-gravity literature there is a large amount of work on the theory and phenomenology of violations of Lorentz invariance (see, *e.g.*, the recent Refs. [7, 8, 36, 37], which also provide a good starting point for a literature search backward in time).

where m_i denotes the mass of the particle with momentum p_i and the fact that p_1 (and, as a consequence, p_2 and p_3) is a large momentum has been used to approximate the square root.

The threshold conditions are usually identified by transforming this laboratory-frame relations into CM-frame relations and imposing that the CM energy be equal to $m_2 + m_3$; however, in preparation for the discussion of deformations of Lorentz invariance it is useful to work fully in the context of the laboratory frame. There the threshold value $p_{1,th}$ of the momentum p_1 can be identified with the requirement that the solutions for p_2 and p_3 as a function of p_1 (with a given value of ϵ) that follow from Eqs. (2), (3) and (4) should be imaginary for $p_1 < p_{1,th}$ and should be real for $p_1 \geq p_{1,th}$. This straightforwardly leads to the threshold equation

$$p_{1,th} \simeq \frac{(m_2 + m_3)^2 - m_1^2}{4\epsilon} \ . \tag{5}$$

This standard Lorentz-invariant analysis is modified [9, 11, 12, 13, 14, 35] by the deformations codified in (1). The key point is that Eq. (4) should be replaced by

$$\epsilon = q + \eta \frac{q^{1+\alpha}}{2E_p^\alpha} \ , \quad E_i \simeq p_i + \frac{m_i^2}{2p_i} + \eta \frac{p_i^{1+\alpha}}{2E_p^\alpha} \ . \tag{6}$$

Combining (2), (3) and (6) one obtains a deformed equation describing the p_1-threshold:

$$p_{1,th} \simeq \frac{(m_2 + m_3)^2 - m_1^2}{4\epsilon} + \eta \frac{p_{1,th}^{2+\alpha}}{4\epsilon E_p^\alpha} \left(\frac{m_2^{1+\alpha} + m_3^{1+\alpha}}{(m_2 + m_3)^{1+\alpha}} - 1 \right) \ . \tag{7}$$

where we have included only the leading corrections (terms suppressed by both the smallness of E_p^{-1} and the smallness of ϵ or m were neglected).

4.2 Phenomenology

Early phenomenological interest in the proposal (1) came from studies based on time-of-flight analyses [31, 15, 16] of photons associated with gamma-ray bursts or with Mk 421. According to (1) (and assuming that there is no leading-order deformation of the standard relation $v = dE/dp$) one would predict [31, 32] energy-dependent relative delays between the times of arrival of simultaneously emitted massless particles:

$$\frac{\Delta T}{T} = \eta \frac{(\alpha + 1)}{2} \frac{E'^\alpha - E^\alpha}{E_p^\alpha} \ , \tag{8}$$

where T is the (average) overall time of travel of simultaneously emitted massless particles and ΔT is the relative delay between the times of arrival of two massless particles of energies E and E'. The fact that such time delays have not yet been observed allows us to set bounds on the α, η parameter space. In particular, data showing (approximate) simultaneity of arrival of TeV photons from Mk 421 were used [16] to set the bound $|\eta| < 3 \cdot 10^2$ for $\alpha = 1$. The same data were used in Ref. [34] to set a more general α-dependent bound on η.

We combine these existing bounds with the assumption that indeed the UHECR and TeV-γ threshold anomalies are due to LID (1). The fact that the scale E_p is very high might give the erroneous impression that the new term going like $p_{1,th}^{2+\alpha}/E_p^\alpha$ present in Eq. (7) could always be safely neglected, but this is not the case [9, 11, 12, 13, 14, 35]. For given values of α, η one finds values of ϵ that are low enough for the "threshold anomaly" [35] (displacement of the threshold) to be significant. For certain combinations α, η, ϵ the threshold completely

disappears, *i.e.* Eq. (7) has no solutions. Assuming (7) one would predict dramatic departures from the ordinary expectations of Lorentz invariance; in particular, if $\alpha \sim -\eta \sim 1$, according to (7) one would expect that the Universe be transparent to TeV photons. The corresponding result obtainable in the UHECRs context would imply that the GZK cutoff could be violated [12] even for much smaller negative values of η. Positive values of η would shift the thresholds in the opposite direction (*e.g.* they would imply an even stricter limit than the GZK one) and are therefore not consistent with the hypothesis that UHECR and TeV-γ threshold anomalies be due to LID (1).

In Figure 1 we provide a quantitative description of the region of the α, η parameter space which would provide a solution to both the UHECR and TeV-γ threshold anomalies while satisfying the time-of-flight constraints [15, 16] that are still consistent with ordinary Lorentz invariance. The curve describing the time-of-flight constraints was obtained using the information that there is [16] an upper bound of order 200 seconds to the difference in time of arrivals of 2TeV photons and 1TeV photons simultaneously emitted by Mk 421 (at redshift of 0.031). The two threshold-anomaly curves reported in Figure 1 were obtained using Eq. (7) with $m_1 = 0$ and $m_2 = m_3 = 5{\cdot}10^5$eV (TeV photons $\gamma + \gamma \to e^+ + e^-$ threshold analysis) and with $m_1 = m_2 = 9.4{\cdot}10^8$eV and $m_3 = 1.4{\cdot}10^8$eV (UHECR $p + \gamma \to p + \pi$ threshold analysis[3]). In light of the analysis of the experimental situation provided in Sections 2 and 3, we obtained the UHECRs curve by requiring sufficient LID to explain the factor-6 threshold shift $5{\cdot}10^{19}$eV$\to 3{\cdot}10^{20}$eV, while for the TeV photons curve we required a factor-2 threshold shift 10TeV $\to$ 20TeV. Even though the shift is more significant in the UHECR context, it is the requirement to explain the TeV-γ threshold anomaly that provides a more stringent constraint, as one should expect since in our LID, which is motivated by Planck-scale physics, the violation of ordinary Lorentz invariance is suppressed by some power of the ratio E/E_p.

Considering the diverse origin and nature of the three relevant classes of experimental data that we are considering, the fact that there is a region of the α, η parameter space consistent with all these constraints is non-trivial, and this in turn provides encouragement for the interpretation of the threshold anomalies as manifestations of LID. Moreover, it is quite striking that this region of parameter space, in spite of being relatively small, does contain one of the two mentioned quantum-gravity-motivated scenarios: $\alpha = 1$ and $1 < \eta < 10^3$. The other quantum-gravity-motivated scenario, the one with $\alpha = 2$ and $1 < \eta < 10^6$, is outside the relevant region of parameter space, being consistent with the absence of relative time delays and the UHECR threshold anomaly but being inconsistent with threshold anomaly for multi-TeV photons.

Concerning the consistency of the interpretation of the threshold anomalies as manifestations of LID it is also important to observe that the modified dispersion relation (1), in spite of affecting so significantly the GZK and TeV-γ thresholds, does not affect significantly the processes used for the detection of the relevant high-energy particles. For the significance of the threshold modification a key role is played, as evident from equation (7), by the smallness of the energy of the background photons. The effect of (1) on atmospheric interactions of the relevant high-energy particles is instead suppressed by the fact that in these atmospheric interactions the "targets", nuclei or electrons, have energies much higher than those of the background photons.

[3]The dominant contribution to the GZK cutoff actually comes from the Δ resonance, so one might find appropriate to replace the sum of the proton mass and the pion mass with the mass of the Δ in the UHECR threshold formula. However, the difference between m_Δ and $m_p + m_\pi$ would only introduce a relatively small correction in our UHECR limit which is not our dominant lower limit (a much stricter limit comes from the TeV-γ anomaly). Moreover, once the contribution to GZK from the Δ is avoided one would still have a (weakened) GZK cutoff from non-resonant photopion production and this would anyway lead to the limit we use.

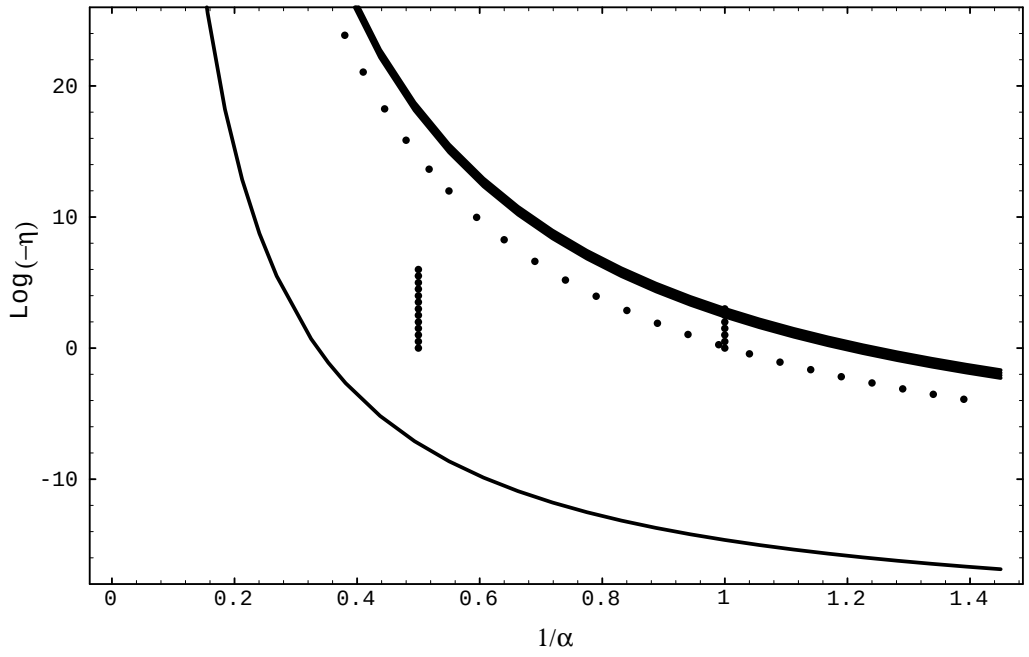

Figure 1: The region of the α, η parameter space that provides a solution to both the UHECR and TeV-γ threshold anomalies while satisfying the time-of-flight upper bound on LID. Only negative values of η are considered since this is necessary in order to have upward shifts of the threshold energies, as required by the present paradoxes. The solid thick line describes the time-of-flight upper bound. The region above this line is excluded. The solid thin line and the dotted line describe the lower bound on LID obtained from the present UHECR (solid thin line) and TeV-γ (dotted line) threshold anomalies. The anomalies disappear in the region above the lines. Within the narrow region between the dotted line and the solid thick line the time of flight constraint is satisfied and both anomalies are resolved. The two vertical segments at $\alpha = 1$ and at $\alpha = 2$ (*i.e.* at $1/\alpha = 1/2$) correspond to the two favored quantum-gravity scenarios. The behaviour of the curves for upper and lower bounds on LID with respect to the bottom-left corner of the frame can be understood by noticing that at a fixed α ordinary Lorentz invariance can be reached taking the $\eta \to 0$ limit, while at fixed η this requires taking the $\alpha \to \infty$ (*i.e.* the $1/\alpha \to 0$) limit.

5 A more general LID formalism

Having shown that the simple two-parameter family of Lorentz-invariance-violating dispersion relations (1) provides a solution of the UHECRs and TeV-γ threshold paradoxes, we turn now to a more general five-parameter LID formulation. The motivation for this formulation comes primarily from theory work on short-distance (so called, "quantum gravity") properties of space-time, in which modifications of space-time symmetries are encountered quite naturally. In particular, quantum-gravity effects inducing some level of nonlocality or noncommutativity would affect even the most basic flat-space continuous symmetries, such as Lorentz invariance. This has been recently emphasized in various quantum-gravity approaches [31-33,39-50] based on critical or noncritical string theories, noncommutative geometry or canonical quantum gravity. While we must be open to the possibility that some symmetries are completely lost, it appears plausible that some of them are not really lost but rather replaced by a Planck-scale-deformed version. Some mathematical frameworks which could consistently describe such deformations have emerged in the mathematical-physics literature [33, 38, 39, 44, 51]. An example of these structures is discussed in Appendix A.

5.1 The five-parameter formalism

The fact that a simple two-parameter family of Lorentz-invariance-violating dispersion relations (1) is consistent with all available data is of course of encouragement for the LID hypothesis, but, especially since relevant data are expected to improve rapidly in the coming years, it is also important to establish how much room for generalizations of (1) is available in the general framework of Planck-scale-induced LID.

One way to generalize (1) would involve attributing different independent values of α, η to different particles. We shall not pursue this (however phenomenologically viable) possibility, since the focus of the present article is on deformations of Lorentz symmetry which could be induced by non-trivial space-time structure, and such deformations would most likely treat "democratically" all particles. In any case, it is clear that models attributing different independent values of α and η to each particle end up having a very large number of free parameters and available data will not be very effective in constraining such models. We shall come back to this point in Section 6, where we consider the alternative (Planck-scale independent) Coleman and Glashow [8] scheme for Lorentz-invariance-violation. In fact, that scheme corresponds to the choice $\alpha = 0$ and an independent value of η for each particle.

Another way to generalize the dispersion relation (1) is to include other deformation terms. In a space-time with some non-trivial structure at distances of order E_p^{-1} one could expect that probes with energy much smaller than E_p should obey a dispersion relation of type:

$$E^2 - p^2 - m^2 = F(E, p, m; E_p) \ , \tag{9}$$

where F is some general function with units of mass (or energy) squared and such that $F \to 0$ for $E_p \to \infty$. Actually, in studies, such as ours, looking only for the leading correction, one of the arguments of F can be suppressed: one makes a subleading error by using $E^2 - p^2 - m^2 = 0$ to express one of the variables in F in terms of the other variables. One could for example express F as a function of p and m only: $F(p, m; E_p)$. Moreover, the fact that we are only looking for the leading correction in the high-energy regime[4] allows us to approximate F with its leading (if any) power dependence on E_p and (within a given power dependence on

[4]It is perhaps worth emphasizing that the low-energy expansion of $F(p, m; E_p)$ may look quite different from its corresponding high-energy expansion. In the high-energy regime ($p \gg m$) the premium is on the leading dependence on p while in the low-energy regime ($p \ll m$) the leading dependence on m is dominant.

E_p) leading dependence on p: $F(p,m;E_p) \simeq \eta\, p^{2+\alpha-\sigma}\, m^\sigma\, E_p^{-\nu}$. In the high-energy regime there is therefore scope for considering the three-parameter family of dispersion relations

$$E^2 - p^2 - m^2 \simeq \eta{\cdot}p^{2+\alpha-\sigma}{\cdot}m^\sigma{\cdot}E_p^{-\alpha}\ , \tag{10}$$

where, of course, it is understood that $m^\sigma = 1$ whenever $\sigma = 0$, even when $m = 0$. (The parameter σ has been introduced to characterize the type of dependence of the deformation term on the mass m, and therefore in our notation there is the implicit prescription that $m^\sigma \to 1$ in the formally ambiguous combined limit $\sigma \to 0$, $m \to 0$.)

Besides the structure of the dispersion relation a LID can also affect the law of sum of momenta. Since our emphasis is here on the phenomenology of LIDs, rather than on their formal/mathematical analysis, we limit our discussion of the motivation for this type of effect to the example of non-commutative geometry (the "κ-Minkowski space-time") considered in Appendix A. As that example clarifies, it is natural to consider a two-parameter class of modifications of the law of sum of (parallel) momenta $K_1 + K_2 \to K_1 + K_2 + \delta(K_1 K_2)^{(1+\beta)/2} E_p^{-\beta}$. For our threshold analyses this corresponds to

$$p_1 - \epsilon \to p_1 - \epsilon - \delta\frac{(p_1\epsilon)^{(1+\beta)/2}}{E_p^\beta} \simeq p_1 - \epsilon\ , \quad p_2 + p_3 \to p_2 + p_3 + \delta\frac{(p_2 p_3)^{(1+\beta)/2}}{E_p^\beta}\ . \tag{11}$$

Overall we consider a five-parameter space: α, η, σ for the dispersion relation and β, δ for the description of possible deformations (11) of the law of addition of momenta. The analysis reported in the preceding Section corresponds of course to the $\sigma \to 0$, $\delta \to 0$ limit of this more general five-parameter $(\alpha, \eta, \sigma, \beta, \delta)$ phenomenology.

As appropriate for the present preliminary status of the experimental situation and the fact that the two-parameter phenomenology analyzed in the previous Section turned out to give a fully satisfactory description of the data, we shall only provide here a preliminary and partial exploration of the enlarged five-parameter space. Our exploration of this parameter space will also be more detailed in some directions and less detailed in others. In particular, we shall limit our analysis to two classes of scenarios, one with $\sigma = 0$ and one with $\sigma = 2, \delta = 0$. This will be sufficient for a qualitative understanding of how different portions of our five-parameter space compare with the present experimental situation.

Retaining the leading corrections in E_p^{-1}, the threshold analysis in the general five-parameter $(\alpha, \eta, \sigma, \beta, \delta)$ LID scenario leads to the threshold equation:[5]

$$\begin{aligned} p_{1,th} \simeq\ & \frac{(m_2+m_3)^2 - m_1^2}{4\epsilon} + \eta\frac{p_{1,th}^{2-\sigma}}{4\epsilon}\left(\frac{m_2^{1+\alpha} + m_3^{1+\alpha}}{(m_2+m_3)^{1+\alpha-\sigma}} - m_1^\sigma\right)\left(\frac{p_{1,th}}{E_p}\right)^\alpha \\ & -\delta\frac{p_{1,th}^2}{2\epsilon}\left(\frac{\sqrt{m_2 m_3}}{m_2+m_3}\right)^{1+\beta}\left(\frac{p_{1,th}}{E_p}\right)^\beta\ . \end{aligned} \tag{12}$$

In the following sections we apply this equation to several specific cases. To simplify the discussion we provide here explicit expressions for the threshold for photopion production:

[5]Note that actually the threshold is not necessarily anomalous; in particular, as we already observed in Ref. [35], when $\alpha = \beta = 1$, $\sigma = 0$ and $\eta = -\delta$ there is a cancellation and the deformed symmetries lead to the same threshold equation obtained with undeformed symmetries.

$$E_{GZK,th} \simeq \frac{7\times10^{19}\ \mathrm{eV}}{\epsilon/0.001\mathrm{eV}}\Big[1+\eta\ 10^{22.2-10.9\sigma-8.15\alpha}\left((0.87^{1+\alpha}+0.13^{1+\alpha})1.15^{\sigma}-1\right)\left(\frac{E_{GZK,th}}{7\times10^{19}\mathrm{eV}}\right)^{2-\sigma}\left(\frac{E_{GZK,th}/7\times10^{19}\mathrm{eV}}{E_p/10^{19}\mathrm{GeV}}\right)^{\alpha} - \delta\ \ 10^{22.1-8.15\beta}\left(\frac{E_{GZK,th}}{7\times10^{19}\mathrm{eV}}\right)^{2}\left(\frac{E_{GZK,th}/7\times10^{19}\mathrm{eV}}{E_p/10^{19}\mathrm{GeV}}\right)^{\beta}\Big]\ , \tag{13}$$

and for pair creation threshold:

$$E_{\gamma,th} \simeq \frac{25\ \mathrm{TeV}}{\epsilon/0.01\mathrm{eV}}\left[1+\eta\ 10^{14.8-7.7\sigma-14.6\alpha}\left(2^{\sigma-\alpha}-\delta^{K}_{\sigma,0}\right)\left(\frac{E_{\gamma,th}}{25\mathrm{TeV}}\right)^{2-\sigma}\left(\frac{E_{\gamma,th}/25\ \mathrm{TeV}}{E_p/10^{19}\mathrm{GeV}}\right)^{\alpha} - \delta\ 10^{14.8-14.9\beta}\left(\frac{E_{\gamma,th}}{25\mathrm{TeV}}\right)^{2}\left(\frac{E_{\gamma,th}/25\ \mathrm{TeV}}{E_p/10^{19}\mathrm{GeV}}\right)^{\beta}\right]\ , \tag{14}$$

where we found convenient to introduce the "Kronecker delta", here denoted with δ^K to differentiate it from our parameter δ, to compactly write this equation consistently with our conventions for the $m_1 \to 0$ limit. [In deriving Eq. (14) from Eq. (12) it is necessary to take into account that, consistently with the conventions and notations we introduced (see, in particular, the comments made immediately after Eq. (10)), in the limit $m_1 \to 0$ the term m_1^σ must be handled according to $m_1^\sigma \to 0$ if $\sigma \neq 0$ and according to $m_1^\sigma \to 1$ if $\sigma = 0$. Of course, the reader can verify by direct calculation that this prescription gives the correct threshold conditions that follow from Eq. (10) in the two cases $\sigma = 0$ and $\sigma \neq 0$, and reproduces the threshold condition (7) obtained in the preceding Section (which was devoted to the case $\sigma = 0, \delta = 0$).]

5.2 Phenomenology with $\sigma = 2, \delta = 0$

In the case $\sigma = 2, \delta = 0$ there is no deformed law of addition of momenta and the threshold equation takes the form

$$p_{1,th} \simeq \frac{(m_2+m_3)^2-m_1^2}{4\epsilon} + \eta\frac{p_{1,th}^{\alpha}}{4\epsilon E_p^{\alpha}}\left(\frac{m_2^{1+\alpha}+m_3^{1+\alpha}}{(m_2+m_3)^{\alpha-1}} - m_1^2\right)\ . \tag{15}$$

For $\sigma \neq 0$ the LID term in (10) vanishes for massless particles. Thus, in general in all $\sigma \neq 0$ cases (like the one we discuss in this Subsection) the time of flight constraints [15, 16] do not limit the LID parameters.

The constraints obtainable by interpreting the UHECR and TeV-γ threshold anomalies as manifestations of LID suggest that this interpretation is quite unnatural in the case $\sigma = 2, \delta = 0$. The condition that both threshold be pushed upwards leads to the constraints $\eta > 0$, $\alpha < 1.195$. Moreover, in order to describe the threshold anomaly for multi-TeV photons one should also make the awkward requirement $\eta > 10^{15\alpha}$. Having provided in the previous section an elegant solution of the threshold paradoxes using $\sigma = 0$ we do not pursue further this scenario which appears to require a higher level of fine tuning.

Scenarios with $\sigma \neq 0$ might regain some interest if there are significant new developments in the understanding of the threshold anomalies that will point in this direction. In the present experimental and theoretical situation we find appropriate to make in the following the assumption that $\sigma = 0$.

5.3 General aspects of the phenomenology with $\sigma = 0$

For $\sigma = 0$ one is left with a four-parameter space on which significant information can be gained by combining data on possible time of flight delays, which will only constrain, through the prediction (8), the parameters α, η, and data on the threshold anomalies, which, through (12), are relevant for all four parameters $\alpha, \eta, \beta, \delta$.

It is important to observe that positive (discovery) results on both the thresholds and the time delays would allow to determine the values of all four parameters. If eventually the mentioned time delays are actually observed, and if they are observed in signals from a collection of sources diverse enough to allow the determination of the energy dependence of the time delays, we would then be able to use (8) to fix α and η. Then, knowing α and η, a determination of the thresholds could be used to fix β and δ.

While waiting for these eventual discoveries, one can use the present upper limits on LID in relative time delays and (preliminary evidence of) lower limits on LID in threshold anomalies to reduce the allowed portion of the four-parameter space. We subdivide the discussion of this type of phenomenological analysis in three cases: $\alpha < \beta$, $\alpha = \beta$ and $\alpha > \beta$.

5.4 Phenomenology with $\alpha < \beta$ (and $\sigma = 0$)

The case $\alpha < \beta$ (and $\sigma = 0$) is essentially analogous to the case considered in the preceding Section with the two-parameter α, η phenomenology. In fact, for $\alpha < \beta$ the threshold corrections associated with the deformation of the law of addition of momenta are suppressed by factors of order $(E/E_p)^{\beta-\alpha}$ with respect to the threshold corrections associated with the deformed dispersion relation. The constraints derived for α, η in the preceding Section would still be valid and, as long as we have only lower or upper limits (rather than definite discoveries), no constraint could be put on β, δ.

5.5 Phenomenology with $\alpha = \beta$ (and $\sigma = 0$)

For $\alpha = \beta$ (and $\sigma = 0$) the upper limit on time-of-flight LID still constrains only α, η, but the constraints on α, η obtainable by interpreting the UHECR and TeV-γ threshold anomalies as manifestations of LID are weakened by allowing also a deformed law of addition of momenta. In practice the parameters α, η and β, δ can in a sense "share the burden" of explaining the threshold anomalies. To illustrate this mechanism we show in Figure 2 the constraints on η, δ that are obtained for $\alpha = \beta = 1$ (and $\sigma = 0$).

5.6 Phenomenology with $\alpha > \beta$ (and $\sigma = 0$)

For $\alpha > \beta$ (and $\sigma = 0$) the threshold corrections associated with the deformed dispersion relation are suppressed by factors of order $(E/E_p)^{\alpha-\beta}$ with respect to the threshold corrections associated with the deformation of the law of addition of momenta. Therefore the interpretation of the UHECR and TeV-γ threshold anomalies as manifestations of LID imposes constraints (lower bounds on LID) on the parameters β, δ. As always, the upper limit on time-of-flight LID constrains only α, η. It is worth noticing that if future data should indicate that there is no LID relative time-delay effect but there are LID threshold anomalies this scenario with $\alpha > \beta$ would become favored.

Figure 3 depicts the limits on β, δ that follow, when $\alpha > \beta$, from interpreting the UHECR and TeV-γ threshold anomalies as manifestations of LID. The limits on α, η due to the upper limit on time-of-flight LID are still the same as in Figure 1 (but, as just mentioned, the two threshold-anomaly curves in Figure 1 do not apply when $\alpha > \beta$).

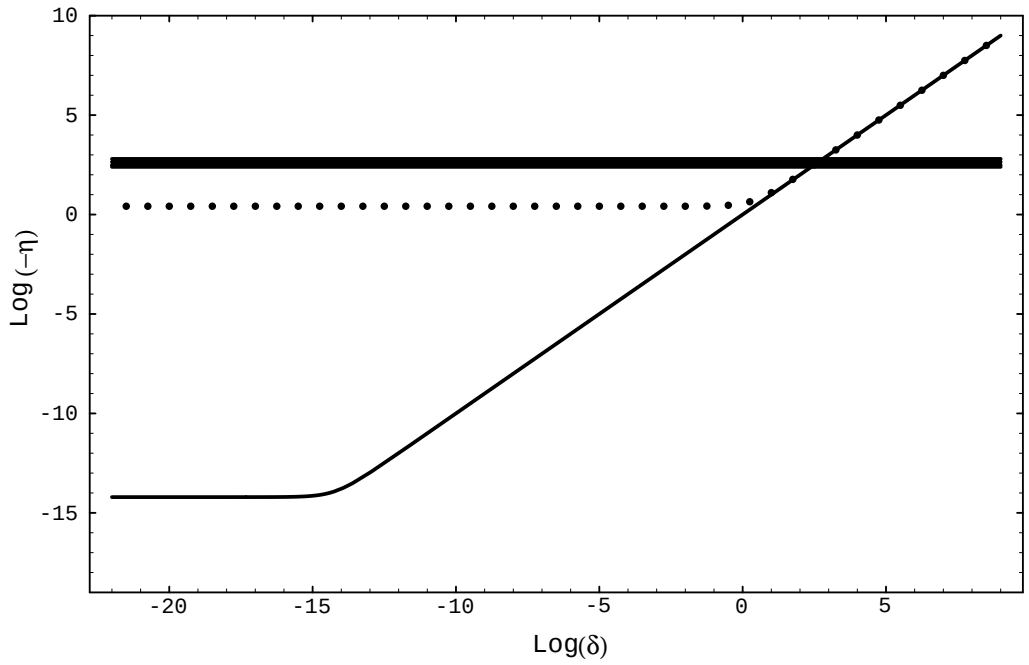

Figure 2: A two-dimensional slice through the five-dimensional parameter space. Shown is the $\eta < 0$ and $\delta > 0$ region for $\alpha = \beta = 1$ and $\sigma = 0$. Analogous considerations (with exchange of roles between η and δ) also apply to the corresponding $\eta > 0$ and $\delta < 0$ region. As in Figure 1, the thick solid line describes the time-of-flight upper bound, while the tentative lower bounds on LID that can be obtained from the present UHECR and TeV-γ threshold anomalies are described by the thin solid line and the dotted line respectively. Notice that for $\delta < 10^{-14}$ the range of allowed η values is almost unaffected by δ, while values of δ such that $\delta > 10^{2.4}$ are not consistent with the working hypothesis of the present Article: the tentative threshold-anomaly lower bound is higher than the time-of-flight upper bound for $\delta > 10^{2.4}$.

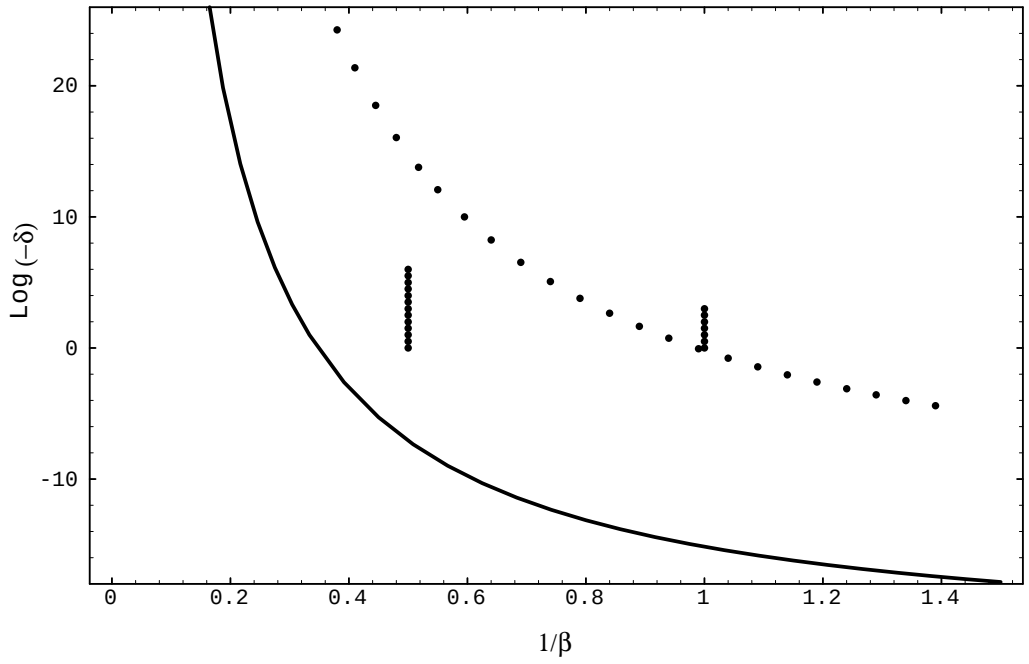

Figure 3: The region of the β, δ parameter space that provides a solution to both the UHECR and TeV-γ threshold anomalies for $\alpha > \beta$. Only negative values of δ are considered since, when $\alpha > \beta$, this is necessary in order to have upward shifts of the threshold energies, as required by the present paradoxes. As in Figure 1, the tentative lower bounds on LID that can be obtained from the present UHECR and TeV-γ threshold anomalies are described by the thin solid line and the dotted line respectively.

6 Comparison with the Coleman-Glashow scheme

Coleman and Glashow [8] have recently introduced a different scheme (denoted CG scheme hereafter) for violation of Lorentz invariance. Modifying the elementary particles Lagrangian they suggest a scheme in which there is a different maximum attainable velocity, c_a, for each particle. The relevant dispersion relations take the form

$$E^2 - p^2 c_a^2 = m^2 c_a^4 \ , \tag{16}$$

where the index a labels the particle. In the language developed in Sections 4 and 5 these dispersion relations (16) involve two terms, one with $\alpha = 0$ and $\sigma = 0$ and the other with $\alpha = 0$ and $\sigma = 2$. The particle-dependence of c_a could be described by allowing for a different independent value of η for each fundamental particle. At high energies, in which we are interested, the $\alpha = 0, \sigma = 0$ term dominates and $\eta_a = c^2 - c_a^2 \approx 2c(c - c_a)$. The condition $\alpha = 0$ reflects the fact that the CG scheme is not motivated by Planck-scale physics. The possibility for each particle to get its own independent value of η reflects the fact that this scheme is not intended as a description of deformations of Lorentz invariance due to non-trivial short-distance space-time structure. (If a deformation of Lorentz symmetry is induced by the structure of space-time we expect that it would affect all particles in the same way. Such a symmetry deformation might allow for a dependence of the correction terms on the mass and the spin of the particle but the parameters of the model should not depend on the mass, spin or other quantum numbers of the particles.)

Using again the language we developed in Sections 4 and 5 one can also give an intuitive characterization of the way in which the CG scheme and the scheme considered here are alternative to one another as strategies for obtaining threshold anomalies. In fact, in that language one could describe undeformed thresholds[6] as associated with $\alpha = 0, \sigma = 0, \delta = 0$, independently of the value of η. This corresponds to the fact that in the CG scheme there are of course no threshold anomalies if all c_a's take the same value ($c_a = c - \eta/(2c)$). Threshold anomalies are generated in the CG scheme by deforming the threshold conditions in the direction that corresponds to keeping $\alpha = 0, \sigma = 0, \delta = 0$ but allowing different independent values of c_a for each fundamental particle. On the contrary, in our scheme the threshold anomalies are obtained by allowing for deviations from $\alpha = 0, \sigma = 0, \delta = 0$ while keeping a single (particle-independent) η.

In light of these comments it is not surprising that threshold anomalies within the CG scheme take the characteristic "$c_a - c_b$" dependence. In particular, as already observed in Ref. [8], the description of the UHECR threshold anomaly requires (together with conditions on $c_\Delta - c_p$) that $c_\pi - c_p > 10^{-24}$. (c_π and c_p are the c_a's for pions and protons respectively.) We observe that a resolution of the TeV-γ threshold anomaly within the CG scheme requires the additional condition $c_e - c_\gamma > 5{\cdot}10^{-16}$. This combines with the absence [8] of vacuum Cerenkov radiation by electrons with energies up to 500GeV in such a way that $c_e - c_\gamma$ is bound to $5{\cdot}10^{-16} < c_e - c_\gamma < 5{\cdot}10^{-13}$. There is therefore a relatively narrow range of allowed values for $c_e - c_\gamma$ just like[7] we found in Section 4 a relatively narrow allowed region of the α, η parameter space.

---

[6] The fact that there are no UHECR and TeV-γ threshold anomalies in our scheme for $\alpha = 0, \sigma = 0, \delta = 0$ can be easily derived directly from the corresponding dispersion relation. This is also implicit in Figure 1, which shows that $|\eta| \to \infty$ as $\alpha \to 0$. Also notice that undeformed thresholds are not only obtained for $\alpha = 0, \sigma = 0, \delta = 0$: the thresholds become undeformed also, for example, in the limit $\alpha \to \infty$ approached keeping $\sigma = 0, \delta = 0$. However the undeformed-threshold point $\alpha = 0, \sigma = 0, \delta = 0$ is best suited for a comparison between our scheme and the CG scheme.

[7] Note however that, while the TeV-γ threshold anomaly is used in both, not all the experimental constraints used by the two phenomenological analysis are the same. In particular, the time-of-flight upper bound on LID was not used to establish $5{\cdot}10^{-16} < c_e - c_\gamma < 5{\cdot}10^{-13}$.

One important difference between the two schemes is that in our Planck-scale-motivated LID the allowed region of parameter space is found exactly where quantum-gravity intuition would have sent us searching for new physics, while in the CG scheme values of $c_e - c_\gamma$ in the range $5{\cdot}10^{-16} < c_e - c_\gamma < 5{\cdot}10^{-13}$ do not have any special significance. Another important difference between the two schemes is that while the same α, η parameters of our scheme for LID are also constrained by UHECR threshold data, in the CG scheme $c_e - c_\gamma$ does not play any role in the equation for the UHECR threshold and vice versa. Any future development in the UHECR threshold data would leave $c_e - c_\gamma$ unaffected. On the contrary, the plausibility of the Planck-scale-motivated LID will be strongly affected by future UHECR threshold data: if the lower limit on the threshold continues to be pushed higher the overall consistency and appeal of the LID model would increase, while the discovery of the threshold not much higher than the present $3{\cdot}10^{20}$eV lower limit would (unless the TeV-γ threshold anomaly is eventually understood as a result of systematic errors) rule out the model considered in Section 4.

While the scheme considered here is more tightly constrained by high-energy data (because all high-energy data set constraints to the same few space-time related parameters), the CG scheme is constrained more tightly than ours by low-energy data. The parameters we considered in the present Article, dealing exclusively with the high-energy regime, are practically unconstrained by low-energy data since, as discussed in Section 5, the LID we considered here might emerge in quantum gravity as the leading order in the high-energy expansion of an analytic function whose low-energy expansion looks quite different. On the contrary the CG scheme takes a fixed (energy-independent) value of its parameters c_a and therefore high-energy and low-energy data can be combined to obtain stricter limits.

7 Summary and outlook

In the present Article we took as working assumption that the UHECR and TeV-γ threshold anomalies do not have a simple explanation (whereas, especially for the case of TeV photons, it might still be legitimate to explore the possibility that systematic experimental errors be responsible for the paradox, and other solutions exist for the GZK paradox) and we attempted to test the plausibility of a description of the anomalies in terms of a Planck-scale-induced deformation of Lorentz symmetry. The results reported in Section 4 certainly indicate that this description is plausible. Had we not been considering such a dramatic departure from conventional physics, we would have probably gone as far as stating that the LIDs we considered provide a compellingly simple description of the anomalies. We do feel that the results of Section 4, also taking into account that there is no other known common explanation of the two threshold paradoxes, provide motivation for additional theory work on the speculative idea of LID and for additional experimental studies aimed at testing the class of Planck-scale-induced LID here considered.

While presently-available data do not in any way invite one to look beyond the simplest two-parameter LID examined in Section 4, in preparation for future studies, especially the expected improvement of the experimental input, we have developed in Section 5 a general parameterization that may prove useful for future attempts to constrain (even rule out) Planck-scale-induced LID. We have emphasized the fact that Planck-scale-induced LID, since it should reflect the structure of space-time, can be characterized by a small number of parameters. In the high-energy regime we found that a very general description of (the leading effects of) Planck-scale-induced LID only requires five parameters and we described how the determination of a few thresholds together with measurements of the speed of very-high-energy particles could fix all five parameters. While we have considered a very general class of LID, it should be stressed that we postponed to future studies the analysis of an important class of further generalizations of Planck-scale-induced LID [43]: deformation terms involving a dependence on polarization/spin of the particles.

In closing we would also like to emphasize the fact that the experimental data here considered represent an important sign of maturity for the general programme of "Planck-length phenomenology" [34, 55]. Whether or not Planck-scale-induced LID turns out to successfully describe future experimental data, the fact that at present we are confronted with experimental paradoxes whose solution could plausibly involve the Planck length, and that certainly the relevant class of observations will eventually be able to rule out various pictures of the short-distance (possibly quantum) structure of space-time, shows that, contrary to popular folklore, some experimental guidance can be obtained for the search of theories capable of unifying gravitation and quantum mechanics. This confirms the expectations, which were based on analyses of the sensitivity of various classes of experiments [52, 31, 53], that emerged from the general quantum-gravity studies reported in Refs. [34, 53, 54, 55] and from analogous studies, primarily focusing on the hypothesis that the unification of gravitation and quantum mechanics should involve non-critical strings, reported in Ref. [56].

We thank Daniele Fargion and Glennys Farrar for many informative discussions on UHECRs.

References

[1] K. Greisen. *Phys. Rev. Lett.*, 16:748, 1966. G. T. Zatsepin and V. A. Kuzmin. *Sov. Phys.-JETP Lett.*, 4:78, 1966.

[2] Nikishov A.I., 1962, Sov. Phys. JETP, 14, 393

[3] Gould J., Schreder G., 1967, PR, 155.5, 1404

[4] Stecker F.W., De Jager O.C. and Salomon M.H., 1992, ApJ, 390L, L49

[5] A. V. Olinto, Phys. Rept. 333-334 (2000) 329-348

[6] M. Harwit, P. J., Protheroe and P. L., Biermann, Ap. J., **524**, L91, 1999.

[7] L. Gonzalez-Mestres, physics/9704017

[8] S. Coleman, S.L. Glashow, Phys. Rev. D59 (1999) 116008.

[9] R. Aloisio, P. Blasi, P.L. Ghia and A.F. Grillo, astro-ph/0001258.

[10] O. Bertolami and C.S. Carvalho, Phys. Rev. D61 (2000) 103002.

[11] H. Sato, astro-ph/0005218.

[12] T. Kifune, astro-ph/9904164, Astrophys. J. Lett. 518 (1999) L21.

[13] W. Kluzniak, astro-ph/9905308.

[14] R. J. Protheroe and H. Meyer, astro-ph/0005349, 2000.

[15] B.E. Schaefer, Phys. Rev Lett. 82 (1999) 4964.

[16] S.D. Biller *et al*, Phys. Rev. Lett. 83 (1999) 2108.

[17] D. J. Bird et al. *Astrophys. J.*, 441:144, 1995.

[18] M. Takeda et al, *Phys. Rev. Lett.*, 81 (1998) 1163.

[19] A. Watson. Proc. Snowmass Workshop, p 126, 1996.

[20] G. Farrar and T. Piran, in preparation, 2000.

[21] F. A., Aharonian, et al., A&A, **349**, 11A, 1999.

[22] Primack J.R., Bullock J.S., Somerville R.S., MacMinn D., 1999, AstroPart., 11, 1-2, 93

[23] Malkan M.A., Stecker F.W., 1998, ApJ, 496, 13

[24] Dwek E., Arendt R.G., 1998, ApJL, 508, L9

[25] S.M Fall, S. Charlot, and Y. C., Pei 1996, ApJ, 464, L43

[26] E. L. Wright, astro-ph/0004192, 2000.

[27] D. P., Finkbeiner, M. Davis and D. J. Schlegel, astro-ph/0004175, 2000.

[28] Hauser M.G., Arendt R.G., Kelsall T. et al., 1998, ApJ, 508, 25

[29] A. Biviano, et al., astro-ph/9910314, 1999.

[30] P. S. Coppi and F. A. Aharonain, astro-ph/9903160, 1999

[31] G. Amelino-Camelia, J. Ellis, N.E. Mavromatos, D.V. Nanopoulos and S. Sarkar, , astro-ph/9712103, Nature 393 (1998) 763.

[32] G. Amelino-Camelia, J. Ellis, N.E. Mavromatos and D.V. Nanopoulos, Int. J. Mod. Phys. A12 (1997) 607.

[33] G. Amelino-Camelia, Phys. Lett. B392 (1997) 283.

[34] G. Amelino-Camelia,, gr-qc/9910089, in: "Towards Quantum Gravity", ed: J. Kowalski-Glikman. Springer-Verlag Heidelberg 2000,

[35] G. Amelino-Camelia and T. Piran, hep-ph/0006210, 2000.

[36] S.M. Carroll, G.B. Field and R. Jackiw, Phys. Rev. D41 (1990) 1231.

[37] R. Jackiw and V.A. Kostelecky, Phys. Rev. Lett. 82 (1999) 3572.

[38] J. Lukierski, A. Nowicki, H. Ruegg, and V.N. Tolstoy, Phys. Lett. B264 (1991) 331; J. Lukierski, A. Nowicki and H. Ruegg, , Ann. Phys. 243 (1995) 90.

[39] G. Amelino-Camelia and S. Majid, hep-th/9907110, Int. J. Mod. Phys. A (in press).

[40] V.A. Kostelecky and R. Potting, Phys. Lett. B381 (1996) 89.

[41] S. Frittelli, C.N. Kozameh, E.T. Newman, C. Rovelli and R.S. Tate, Class.Quant.Grav. 14 (1997) A143.

[42] G. Amelino-Camelia, Mod. Phys. Lett. A13 (1998) 1319.

[43] R. Gambini and J. Pullin, Phys. Rev. D59 (1999) 124021.

[44] G. Amelino-Camelia, J. Lukierski and A. Nowicki, gr-qc/9903066,Int. J. Mod. Phys. A14 (1999) 4575.

[45] J. Alfaro, H.A. Morales-Tecotl, L.F. Urrutia, Phys. Rev. Lett. 84 (2000) 2318.

[46] J. Ellis, K. Farakos, N.E. Mavromatos, V.A. Mitsou and D.V. Nanopoulos, astro-ph/9907340.

[47] L. Smolin, Physics World 12 (1999) 79.

[48] Hong-wei Yu and L.H. Ford, gr-qc/0004063.

[49] T. Thiemann and O. Winkler, hep-th/0005235.

[50] G.Z. Adunas, E. Rodriguez-Milla and D.V. Ahluwalia, Phys. Lett. B485 (2000) 215.

[51] S. Majid and H. Ruegg, Phys. Lett. B334 (1994) 348.

[52] J. Ellis, J.S. Hagelin, D.V. Nanopoulos and M. Srednicki, Nucl. Phys. B241 (1984) 381.

[53] G. Amelino-Camelia, gr-qc/9808029, Nature 398 (1999) 216.

[54] D.V. Ahluwalia, gr-qc/9903074, Nature 398 (1999) 199.

[55] G. Amelino-Camelia, gr-qc/0008010.

[56] J. Ellis, N.E. Mavromatos and D.V. Nanopoulos, Gen. Rel. Grav. 31 (1999) 1257.

Appendix A: κ-Minkowski space-time

In order to illustrate in an explicit framework some of the structures relevant for our analysis of LID, in this Appendix we give a brief descrition of the "κ-Minkowski" non-commutative space-time, which was developed in Refs. [33, 38, 39, 44, 51]. The simplicity of κ-Minkowski, which is basically an ordinary Minkowski space-time on which however one postulates that the time coordinate does not commute with the space coordinates ($[x_i, t] \sim x_i/E_p$), renders it very useful for the purpose of illustrating the new conceptual elements required by space-times with a nontrivial short-distance structure.

A first point that deserves being emphasized is the connection between flat nontrivial space-times and quantum gravity. In quantum gravity one has the general intuition [34, 42] that ordinary classical commutative space-times should emerge from some more fundamental underlying picture. To very compact (Planckian-energy) probes space-time should look completely different from an ordinary classical space-times. On the contrary probes of very low energy should not be affected in any noticeable way by the nontrivial short-distance structure of space-time. In the intermediate regime (mid-energy probes [34, 42]) one would expect to be able to use roughly the same language of ordinary classical space-times, but with the necessity to introduce some new concepts (such as the little element of noncommutativity of κ-Minkowski) reflecting the leading-order effects of quantum-gravity at low energies. This hierarchy of regimes is to be expected not only in high-curvature space-times (where classical-gravity effects are stronger), but also in space-times that appear to be trivial and flat to very-low-energies probes. κ-Minkowski is [42] a model (toy model?) of how a probe of relatively high energy could perceive a space-time that instead appears to be trivially Minkowski to probes of very low energy.

In κ-Minkowski a relation of type (1) can be obtained as a direct consequence of the κ-Poincaré invariance [33, 38, 39, 44, 51] of this space-time. κ-Minkowski therefore provides an example of the mentioned scenario in which an ordinary symmetry is violated but there is no "net loss of symmetries" (the 10-generator Poincaré symmetry is replaced by the 10-generator κ-Poincaré symmetry). It is in order to capture the essence of these situations

that one introduces the terminology "symmetry deformation" (in alternative to "symmetry violation" which could be reserved for cases with a net overall loss of symmetries). In Sections 4 and 5 we denominate our scheme as a LID just to emphasize that the equations we use do not necessarily reflect a loss of symmetry (whether or not they do imply a net loss of symmetry depends on the underlying algebraic structures that lead to those equations in a given space-time picture).

Importantly, consistency with the non-commutative nature of κ-Minkowski space-time also requires [33, 38, 39, 44, 51] that the law of addition of momenta be accordingly modified. This modification emerges at the level of the κ-Poincaré (Hopf) algebra, and of course requires physical interpretation (particle momenta in a noncommutative space-time are a new concept). A prescription suitable for handling the ambiguities due to the non-commutative nature of κ-Minkowski space-time was given recently in Ref. [39], and in the cases here of interest, which always involve the sum of parallel momenta of two particles (at threshold particles are produced at rest in the CM frame), it reduces (in leading order in E_p^{-1}) to the prescription that the sum of momenta K_1 and K_2 can be handled with ordinary algebraic methods upon the replacement $K_1 + K_2 \to K_1 + K_2 + \delta K_1 K_2/E_p$, where δ is a parameter analogous to η. In the analyses reported in Sections 4 and 5 this would imply $p_1 - \epsilon \to p_1 - \epsilon - \delta p_1 \epsilon/E_p$ and $p_2 + p_3 \to p_2 + p_3 + \delta p_2 p_3/E_p$, and actually, since of course we have been here only interested in the leading E_p^{-1} effect and $\epsilon \ll p_2 \sim p_3 \sim p_1$, one can neglect the term of order $p_1\epsilon/E_p$ while retaining the term of order $p_2 p_3/E_p$.